NEOPLASIA
www.neoplasia.com

Volume 22 Number xxx Month 2020 pp. 800–808

Exome sequencing identifies frequent genomic loss of *TET1* in *IDH*-wild-type glioblastoma ☆, ☆☆,1,2

Sebastian Stasik [a]; Tareq A. Juratli [b]; Andreas Petzold [c]; Sven Richter [b]; Amir Zolal [b,d]; Gabriele Schackert [b]; Andreas Dahl [c]; Dietmar Krex [b,†]; Christian Thiede [a,†,*]

[a] Department of Medicine I, Medizinische Fakultät Carl Gustav Carus, Technische Universität Dresden, Dresden, Germany
[b] Department of Neurosurgery, Medizinische Fakultät Carl Gustav Carus, Technische Universität Dresden, Dresden, Germany
[c] DRESDEN-Concept Genome Center, Center for Molecular and Cellular Bioengineering, Technische Universität Dresden, Dresden, Germany
[d] Department of Spine Surgery and Neurotraumatology, SRH Wald-Klinikum Gera, Gera, Germany

Abstract

Glioblastoma (GBM) is the most common and malignant brain tumor in adults. Genomic and epigenomic alterations of multiple cancer-driving genes are frequent in GBM. To identify molecular alterations associated with epigenetic aberrations, we performed whole exome sequencing-based analysis of DNA copy number variations in 55 adult patients with *IDH*-wild-type GBM. Beside mutations in common GBM driver genes such as *TERT*p (76%), *TP53* (22%) and *PTEN* (20%), 67% of patients were affected by amplifications of genes associated with RTK/Rb/p53 cell signaling, including *EGFR* (45%), *CDK4* (13%), and *MDM2/4* (both 7%). The minimal deleted region at chromosome 10 was detected at the DNA demethylase *TET1* (93%), mainly due to a loss-of-heterozygosity of complete chromosome 10 (53%) or by a mono-allelic microdeletion at 10q21.3 (7%). In addition, bi-allelic *TET1* deletions, detected in 18 patients (33%), frequently co-occurred with *EGFR* amplification and were associated with low levels of *TET1* mRNA expression, pointing at loss of TET1 activity. Bi-allelic *TET1* loss was not associated with global concentrations of 5-hydroxymethylcytosine, indicating a site-specific effect of TET1 for DNA (de)methylation. Focal amplification of *EGFR* positively correlated with overall mutational burden, tumor size, and poor long-term survival. Bi-allelic *TET1* loss was not an independent prognostic factor, but significantly associated with poor survival in patients with concomitant *EGFR* amplification. Rates of genomic *TET1* deletion were significantly lower in a cohort of *IDH1*-mutated patients. Despite the relevance of TET1 for DNA demethylation and as potential therapeutic target, a frequent genomic loss of *TET1* has not previously been reported in GBM.

Neoplasia (2020) 22, 800–808

Keywords: Glioblastoma (GBM), Next-generation sequencing (NGS), Copy number variation (CNV), *IDH*, *TET1* deletion, *EGFR* amplification

Introduction

Glioblastoma multiforme (GBM) is the most common malignant brain tumor in adults with dismal prognosis [1]. Despite a combination of surgical resection, adjuvant radiation and chemotherapy with temozolomide in current standard treatment regimens and ongoing research for targeted therapies using specific drugs (e.g., *EGFR* kinase inhibitors), GBM mostly remains incurable with a high mortality rate and a 5-year survival of <6% [2]. Among several factors, a high inter- and intratumoral molecular heterogeneity limits confident predictions on drug resistance and therapy response [3,4].

* Corresponding author.
E-mail address: Christian.Thiede@uniklinikum.dresden.de (C. Thiede).

☆ Funding: This research did not receive any specific grant from funding agencies in the public, commercial, or not-for-profit sectors.

☆☆ Ethics approval and consent to participate: All tumor tissue and blood samples (used as germline control) were collected with written informed consent and after approval by the local ethics committee of the Medical Faculty Carl Gustav Carus Dresden.

[1] Data Statement: All data that support the findings of this study are included in this published article and its supplementary information files.

[2] Declaration of Competing Interest: C.T. is CEO and co-owner of AgenDix GmbH, a company performing molecular diagnostics. T.J. received honoraria from Roche and CSL Behring. The remaining authors declare no conflict of interest.

† DK and CT contributed equally.

Received 20 August 2020; received in revised form 15 October 2020; accepted 16 October 2020

https://doi.org/10.1016/j.neo.2020.10.010

Depending on histopathological and molecular (*IDH1/2* status) features, GBM can be classified into *IDH*-wild-type (wt; ~90% of cases) and *IDH*-mutated GBM [5]. Beside *IDH* mutations, a variety of recurrent genetic aberrations were reported in GBM, including common oncogenic DNA sequence alterations in genes such as *EGFR, PTEN, NF1*, and *TERT* promoter (*TERT*p) as well as large chromosomal aberrations (+7, −10) [6,7]. Moreover, submicroscopic DNA copy number variations (CNV; e.g., at *EGFR, MDM2/4, CDK4, PTEN*, and *CDKN2A/B*) were detected as oncogenic aberrations in GBM, ultimately affecting 3 main cell signaling pathways (p53, Rb, and RTK/Ras/PI3K) that initiate and sustain disease progression [8,9].

In addition to key molecular alterations, GBM can be distinguished based on transcriptional and epigenetic differences [6,7]. For example, *IDH1*-mutated GBM typically harbor other frequent genomic alterations such as mutations of *ATRX* and *TP53* and are characterized by a distinct pattern of DNA hypermethylation via the conversion of α-ketoglutarate (αKG) to 2-hydroxyglutarate (2HG) and subsequent alterations of specific histone marks [10,11]. The production of 2HG inhibits several αKG-dependent oxygenases, including the ten-eleven translocation (TET) enzymes. The TET enzymes act by transcriptional activation or repression of target genes in many cellular processes. For instance, they are the primary mode of active DNA demethylation by catalyzing the re-oxidation of 5-methylcytosine (5mC) to 5-hydroxymethylcytosine (5hmC) [12]. Epigenetic alterations initiated by mutations of *IDH1/2* and/or *TET1/2/3* and subsequent impaired production of 5hmC have been reported in several cancer entities such as myeloid malignancies [13,14].

To identify molecular alterations associated with epigenetic deregulation in *IDH*-wt GBM, we performed whole exome sequencing and evaluated for the presence of recurrent mutations, chromosomal aberrations and CNVs. Patients' clinical characteristics were analyzed according to the mutational status. Hereby, we identified *TET1* as frequently deleted gene, not previously described in The Cancer Genome Atlas (TCGA) database. Moreover, due to the importance of *TET1* for DNA demethylation, we quantified corresponding levels of *TET1* mRNA expression and global concentrations of 5hmC and 5mC as a surrogate measure for total DNA (de)methylation. Finally, to address the overall prevalence of this alteration in more detail we comparatively quantified levels of 5mC/5hmC and rates of genomic *TET1* deletion in a cohort of 20 patients diagnosed with *IDH1*-mutated GBM, using PCR-based analysis of STR microsatellites.

Material and Methods

Patient Characteristics and Sample Collection

This study included a total of 55 patients with newly diagnosed *IDH*-wt GBM who underwent surgical resection at the University Hospital Carl Gustav Carus in Dresden. In addition, 20 patients with *IDH1* mutated GBM were included for *TET1* deletion mapping. All tumor tissue and blood samples (used as germline control) were collected with written informed consent and after approval by the local ethics committee of the Medical Faculty Carl Gustav Carus Dresden. Tumor tissues were taken intraoperatively and were snap frozen at -80°C. Frozen tumor tissue was sectioned using the Cryostat Jung CM 1800 (Leica, Wetzlar, Germany). To assure a tumor cell content of >80% for DNA extraction, a fresh hematoxylin and eosin-stained reference section was re-reviewed by an experienced local neuropathologist. Genomic DNA was isolated using the QIAmp DNA Mini Kit (Qiagen, Hilden, Germany) according to manufacturer's protocols and quantified using NanoDrop 1000 spectrophotometer (Thermo Fisher Scientific, Waltham, MA, USA).

IDH *and* TERT*-Promoter Mutation Detection*

The *IDH1/2* mutational status was determined in tumor tissue prior to exome sequencing by Sanger sequencing, using established primer sets, as published elsewhere [15]. The proximal *TERT* promoter, covering nucleotides C228 and C250, was amplified using a nested PCR procedure and sequenced on an Ion Torrent S5 NGS system, as described previously [16]. Data were analyzed using the Torrent Suite software v3.2 and the Torrent Variant Caller v.4.0 plugin with default settings and alignment to the hg19 human reference genome from the UCSC Genome Browser (http://genome.ucsc.edu/).

Exome Sequencing, Variant Calling, and Filtering

Library preparation and exome enrichment of paired blood and tumor samples from *IDH*-wt patients was performed using the SureSelect QXT and SureSelect Human All Exon V6 + COSMIC (Agilent Technologies, Santa Clara, CA, USA) protocols capturing ~60Mb of exonic targets, according to manufactures protocols. After quantification and quality control using a Qubit 4.0 fluorometer (Life Technologies) and the Agilent 2200 TapeStation (Agilent Technologies), final libraries (mean insert size ~250bp) were sequenced paired-end (2 × 75bp) on an Illumina HiSeq platform. Between 30 and 60 mio reads were generated per sample. Overall enrichment efficiency was ~80% (on-target rate) with high coverage uniformity across all chromosomes. Sequencing depth was >10x for over 99% of sequence regions, reflecting the minimum coverage required for SNV analysis. Superior coverage of >30x and >60x was achieved for over 80% and 50% of the sequence regions, respectively. SNV analysis was performed with GATK [17] following the best practices recommended by the GATK team. Briefly, raw paired-end reads were mapped with BWA to human genome hg19 using default parameters [18] and duplicates were tagged using picardtools (http://broadinstitute.github.io/picard/). Insertions/deletions were realigned and base qualities recalibrated using GATK. Variants were identified for individual samples using the HaplotypeCaller tool of GATK in GVCF mode and genotypes were then jointly called using the GenotypeGVCFs tool of GATK. Annotation and filtering of somatic variants in coding regions was performed using tumor/germline pairs with a defined threshold of 10x (read depth) and a cut-off of 10% variant allele frequency using the VariantStudio software (Illumina Inc., San Diego, CA, USA) and the SeattleSeq Annotation 138 software (University of Washington, Seattle, WA, USA).

Copy Number Variation Detection and GISTIC Analysis

CNV analysis was performed with GATK following the best practices recommended by the GATK team. Briefly, raw paired-end reads were mapped with BWA to human genome hg19 using default parameters and duplicates were tagged with picardtools. The next steps were done with tools of the GATK framework. The sequence regions were divided into 1kb bins and counts per bin were obtained. Counts were corrected for GC, converted into log2 copy ratios (using sample median as baseline) and denoised with a panel of normals built from the count data of the blood samples. Additionally, allelic counts were determined for variant sites. Denoised copy ratios as well as allelic counts were then used to model copy ratio segments (i.e., adjacent bins sharing the same copy ratio). For tumor samples, the allelic counts of the matched blood sample were included as well to infer the original nontumor state of the genome. Finally, CN gains and losses were called for the modeled segments. To identify regions of significant amplification or deletion across the set of tumor samples, the GISTIC [19] module was run with the following parameters: -genegistic 1 -smallmem 1 -broad 1 -brlen 0.5 -conf 0.90 -armpeel 1 -savegene 1 -gcm extreme.

Short Tandem Repeat Analysis

To confirm somatic *TET1* deletion in tumor/normal samples, loss of heterozygosity (LOH) was mapped using PCR-based analysis of short tandem repeat (STR) loci D10S2480 and GATA121A08 (both in close distance to *TET1*, 10q21.3), according to standard protocols on an ABI 3130xl (Life Technologies). PCR was carried out using the Qiagen Multiplex PCR Kit (Qiagen, Hilden, Germany) with following Primer sequences: (for D10S2480) 5'-CTGAGTTAGGGTCTTGCTATG-3' (Forward); 5'-TAAGGAAGACAAACTCATTATTTCC-3' (Reverse) and (for GATA121A08) 5'-GTTAACAGACTATTACCTGCCTACC-3' (Forward); 5'-TGAGTATGCCACACTGCA-3' (Reverse). Additionally, STR analysis was performed in a group of 20 patients diagnosed with *IDH1*-mutated GBM.

TET1 *Expression Profiling*

Total RNA from frozen tumor tissue was isolated using the RNeasy Mini Kit (Qiagen) in a QIAcube (Qiagen) according to manufacturer's protocols. Conversion to cDNA was performed using the SuperScript VILO MasterMix with 11.5 µL of RNA for RT (Invitrogen Corporation, Carlsbad, CA, USA). *TET1* expression was quantified using a custom TaqMan gene expression assay (Thermo Fisher Scientific, ref: 4331182) with gene specific PCR primers and the TaqMan Universal Master Mix on a 7500 qRT-PCR device (Applied Biosystems, Foster City, CA, USA). Levels of *TET1* mRNA were quantified relative to glyceraldehyde-3-phosphate dehydrogenase (*GAPDH*; Delta-CT values) expression as internal control. The 2^(Delta-Delta-Ct) method was used to calculate relative differences of *TET1* mRNA expression between samples, normalized to *TET1*-wt gene expression.

Quantification of 5-methylcytosine and 5-hydroxymethylcytosine

Global concentrations of 5-methylcytosine (5mC) and 5-hydroxymethylcytosine (5hmC) were quantified on genomic DNA of *IDH*-wt and *IDH*-mutated tumors by an ELISA using the MethylFlash Methylated and Hydroxymethylated DNA Quantification Kit (Fluorometric; Epigenetik, Farmingdale, NY, USA) according to the manufacturer's protocol.

Radiological Evaluation and Volumetric Measurements

All patients received a pre- and postoperative MRI with T1, T1 postcontrast, T2, and FLAIR sequences. Radiologic progression was determined using the criteria for Radiologic Assessment in Neuro-Oncology [20]. Additionally, the preoperative T1-weighted postcontrast MR scans were used to measure the enhancing tumor size and obtain volumetric measurements. A combination of manual segmentation using the ITK-SNAP software [21] and intensity filtering based on individually adjusted thresholds was used to select the enhancing tumor tissue with and without the necrotic tumor portion.

Clinical Data and Statistical Analysis

Demographic data, pathological findings and clinical data were retrospectively collected for patients with *IDH*-wt GBMs. Progression-free survival (PFS) was calculated from the day of first surgery until imaging-based detection of tumor progression (or end of follow-up). Overall survival (OS) was defined as the period from the day of first surgery until death (or the end of follow-up). The statistical association of clinical variables (e.g., age, tumor size, rates of somatic variants, survival) was evaluated using the 2-sided Students *t* test and Mann-Whitney *U* test. Survival analysis (PFS and OS) was carried out using the Kaplan-Meier technique. To test for statistical significant differences between survival curves the Mantel-Cox test (Log-rank test) was used. *P* values <0.05 were considered significant. All calculations were conducted using Prism 5 (GraphPad, La Jolla, CA, USA) and SPSS Statistics 25 (IBM, Armonk, NY, USA).

Results

Demographic Characteristics and Pathological Findings

A total of 55 patients (33 male/22 female) with newly diagnosed *IDH*-wt GBM were included. Median age at first diagnosis was 58 y (range 23–80 y; interquartile range 44–73 y). *IDH*-wt classification of tumors was confirmed by Sanger sequencing covering residues R172 (*IDH2*) and R132 (*IDH1*) in all patients. Tumors affected the left (n = 22); right (n = 31) or both hemispheres (n = 2) and were mainly localized in the frontal lobe (n = 18), temporal lobe (n = 13), parietal lobe (n = 3), occipital lobe (n = 2), or in multiple lobes (n = 13). Median tumor size was 43.8 cm^3 (range 0.53–132.89 cm^3) with Ki67 levels ranging between 5% and 90% (median 30%). Methylation of the *MGMT* promoter was detected in 17 tumors (30.9%). Patient's median OS was 14.4 mo (range 2–66 mo). During the time of follow-up, 47 patients (85%) passed away, 3 patients were lost from follow-up and 5 patients were still alive at the last update of disease progression, conducted in January 2020. Significant associations of clinical variables with outcome were observed using median values of Ki67 proliferation marker (21.7 vs 11.5 mo; $P = 0.0002$) and tumor size (17.6 vs 12.0 mo; $P = 0.020$) to dichotomize patients (Figure S1). Moreover, there was a trend towards shorter survival with increasing age ($P = 0.071$). Demographic characteristics and pathological findings of patients are presented in Supplementary Table S1.

Mutational Landscape of Tumors

Overall, after filtering (≥10fold coverage; ≥10% VAF) and exclusion of frequent polymorphisms (>0.1% population frequency), synonymous variants, variants in noncoding regions (intronic and UTRs) and germline variants (based on tumor/blood subtraction), a total number of 1841 somatic mutations in 1544 different genes were detected in the 55 tumor exomes, corresponding to a mean rate of ~33 somatic variants per patient. The majority of mutations (93%) were single nucleotide variants (SNVs) (n = 1719), comprising 1616 missense and 103 nonsense SNVs, followed by frame-shift (n = 76) and in-frame InDel mutations (n = 46). Mutations were detected with a median VAF of 31% (range 10%–98%).

As summarized in Figure 1A, we identified a series of frequently mutated genes (grey bars), including well-known GBM driver genes such as *TERT*p (76%), *EGFR* (29%), *TP53* (22%), *PTEN* (20%), *NF1* (9%), *ATRX* (5%), *PIK3CA* (5%), *PIK3R1* (4%), and *PDGFRA* (4%). Other previously reported candidate genes, recurrently mutated in our cohort (in 2 or more patients) were *LZTR1* (4%), *KIT* (4%), and *KMT2B* (4%). Importantly, we did not detect any *TET1* or *TET2* mutations in our study group. Beside alterations in common recurrent driver genes, most patients carried one or more additional mutations in cancer associated genes functionally linked to transcriptional regulation (e.g., *RB1, RUNX1, CIITA, CNOT3, NCOR1/2, SALL4*), histone modification (e.g., *SETD2*), chromatin-remodeling (e.g., *CREBBP* and *INO80*), the SWI/SNF complex (*SMARCA1*), alternative splicing (e.g., *DDX3X* and *RBM10*), or signaling (e.g., *MET, MTOR, BRAF, ERBB2*; Figure S2). No associations with clinical outcome (PFS/OS) were observed for the mutational status of individual driver genes, including *TERT*p, *EGFR, TP53, PTEN*, and *NF1* (Figure S3).

Profiling of Copy Number Variations

NGS coverage-based assessment of copy number ratios (CNR) in exomes from tumor/blood pairs revealed a median frequency of 152 somatic CNVs

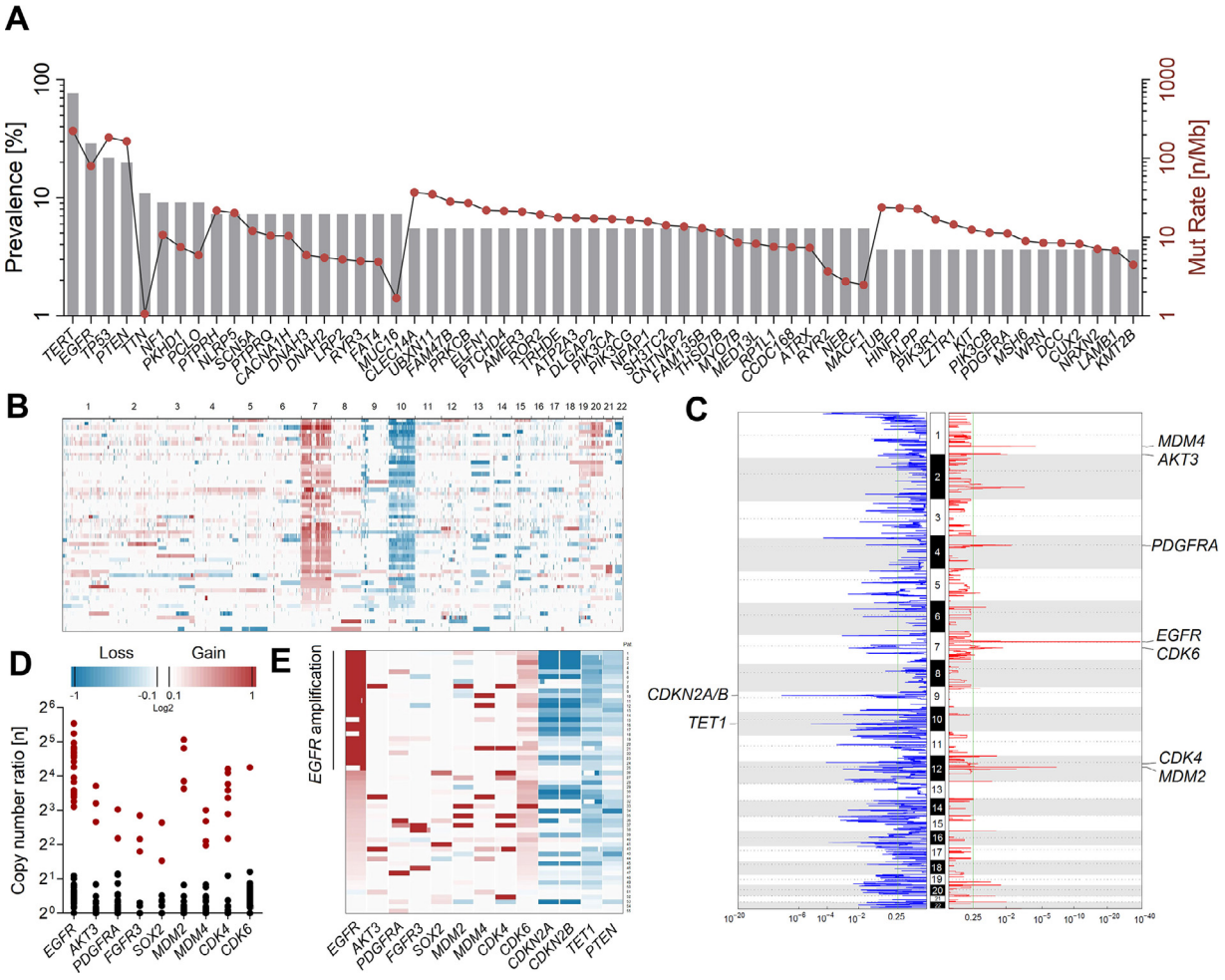

Figure 1. Somatic genomic alterations in *IDH*-wt Glioblastoma. (A) Prevalence (%; gray bars) and mutation rate (n Mb^{-1}; red dots) of frequently mutated genes in coding regions from 55 tumor exomes. Filtering of somatic variants was performed using tumor/germline pairs with a defined cut-off of 10% variant allele frequency (VAF). *TERT* promoter mutations at residues C228 and C250 were analyzed using a targeted NGS procedure (B) Overall genomic copy number variations (CNVs) and chromosomal locations in 55 *IDH*-wt GBM. (C) Recurrent sites of focal amplification (red) and deletion (blue) determined by the GISTIC module. Most significant focal amplification was detected for *EGFR* (chr7; q-value = 6.74E−39). The minimal region of allelic loss at chromosome 10 was detected for *TET1* (q-value = 3.16E−06). All statistically significant (q-value <0.25) regions are summarized in Supplementary Table S2. (D) Copy number ratios (CNR) of genes frequently affected by focal amplification (CNR >2; red dots). (E) Association of the *EGFR* amplification status with genomic gains (red) and losses (blue) in relevant oncogenes.

per patient. Genomic losses accounted for the majority (66%) of detected CNVs (34% gains). Overall, CNV patterns virtually resembled genomic profiles previously reported for *IDH*-wt GBM, including characteristic gains (CNR 1–2) at chromosome 7p (87%) and/or 7q (82%) as well as partial or complete loss-of-heterozygosity (LOH) at chromosome 10p (78%) and/or 10q (85%) including the tumor suppressor *PTEN* (10q23; Figure 1B). Large chromosomal gains also affected chromosomes 19 (18%), 20 (27%), and 21q (11%).

In accordance with the TCGA database, highest rates of focal amplification were detected for *EGFR*, with CNRs ranging between 8 and 46 fold in roughly half of tumors (45%) (Figure 1C and D). Generally, the *EGRF* status was not significantly associated with patient's age (Figure 2A). Amplification of the *EGFR* gene was significantly associated with rates of overall mutational burden (P= 0.0051; Figure 2B), genomic loss of *CDKN2A/B* at 9p21 (P< 0.0001; Figure 2G) and rates of concomitant *EGFR* mutations (P< 0.0001; Figure 2H). In addition, *EGFR* amplification positively correlated with histopathological measures of tumor size (P= 0.0836; Figure 2C), *MGMT* promoter methylation (P= 0.3706; Figure 2F) and Ki67 staining (P= 0.7910; Figure 2D). Generally, *EGFR* amplification was not associated with median PFS and OS of patients (P= 0.2283; Figure 2E). However, obviously *EGFR* amplification correlated with poor long-term survival, irrespective of comparing survival rates at 2 y (33% vs 20%), 3 y (17% vs 0%), or 5 y (7% vs 0%) for patients without or with *EGFR* amplification (Figure 2I).

Almost mutually exclusive to *EGFR* amplifications, other frequent RTK aberrations were detected at *FGFR3* (5%), *PDGFRA* (4%), *AKT3* (5%), and *SOX2* (Figure 1E). Furthermore, focal amplifications in other regulatory pathways affected *MDM2/4* (both 7%), *CDK4* (13%), and *CDK6* (2%; Figure 1D). Mutually exclusive to *CDK4* amplifications, 65% of patients carried typical deletions of *CDKN2A/B* with CNRs clearly <0.5 in the majority of cases (~75%), demonstrating a predominance of homozygous loss at 9p21 (Figure 1C and E). Other cancer associated genes with frequent heterozygous deletions (CNR 0.5–1) were *CDK7* (55%), *RB1* (25%), and *TP53* (13%). The mutational profiles and CNV patterns of *IDH*-wt exomes

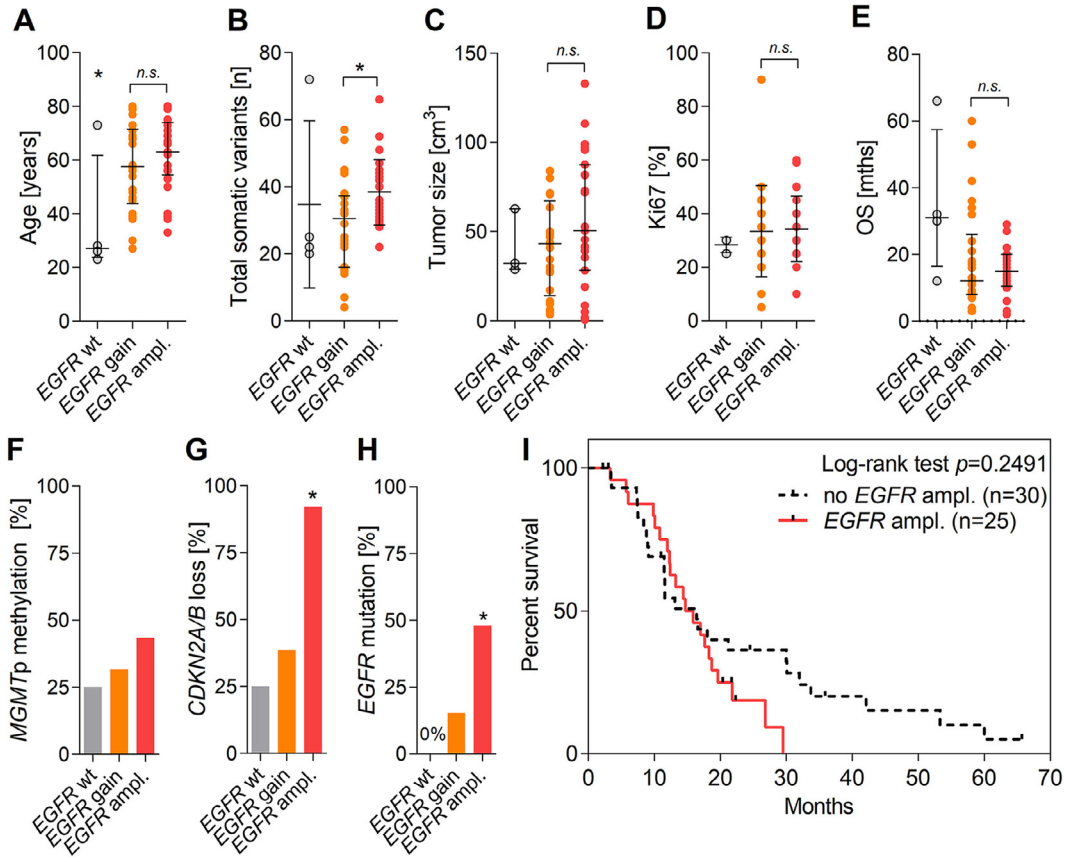

Figure 2. Associations of *EGFR* amplification in *IDH*-wt GBM. (A) Age at diagnosis (y), (B) total amount of somatic mutations (n), (C) tumor size (cm^3), (D) Ki67 value (%), (E) overall survival (mo), (F) *MGMT*p methylation (%), (G) *CDKN2A/B* loss (%) and (H) concomitant *EGFR* mutations (%) in patients with *EGFR*-wt (n = 4), *EGFR* copy number gain (n = 26) and *EGFR* amplification (n = 25). Error bars indicate median values with interquartile range. (I) Kaplan-Meier analysis showing overall survival (mo) of *IDH*-wt patients with (n = 25) or without (n = 30) focal amplification of the *EGFR* gene. Statistical associations were evaluated using the two-sided Students *t* test, the Mann-Whitney *U* test and the Mantel-Cox test. *P* values <0.05 were considered significant.

are shown in Figure 3. A list of all regions affected by significant genomic deletion and amplification detected using GISTIC analysis is presented in Supplementary Table S2.

Frequent Copy Number Loss of TET1

Interestingly, the minimal region of allelic loss at chromosome 10 was detected at 10q21.3, covering a genomic size of ~500 kb (Figures 1C and 4A). This minimal deleted region in our cohort is not listed in the TCGA datasets and affects a series of genes including *RUFY2, DNA2, SLC25A16, CCAR1*, and the DNA demethylase *TET1* (Tet Methylcytosine Dioxygenase 1). Overall, *TET1* deletions were detected in 51 patients (93%) with CNRs ranging between 0.23 and 0.82 (median CNR = 0.58; Figure 3 and Supplementary Table S3). The majority of patients were affected by a heterozygous loss of *TET1* due to the presence of LOH at chromosome 10 (53%). Heterozygous *TET1* deletions in patients without LOH of chromosome 10 were detected in 7% of GBM patients, indicating the presence of submicroscopic micro-deletions at 10q21.3. In addition, *TET1* deletion was detected with CNRs <0.5 in 18 patients (33%) with LOH of chromosome 10, pointing at bi-allelic micro-deletions at 10q21.3 (i.e., not detected at other chr10 regions including genes such as *PTEN*), inducing complete loss of TET1 activity (Figure 4B). STR-based detection of LOH in tumor/blood pairs, using *TET1* microsatellite markers D10S2480 and GATA121A08, confirmed somatic deletion at 10q21.3 in 48 patients with informative results (Supplementary Table S3). LOH detection was not possible in three patients with homozygous STR loci in germline controls. Based on LOH detection using STRs, all bi-allelic *TET1* deletions occurred in *IDH*-wt GBM, whereas only 35% of *IDH1*-mutated GBM harbored a mono-allelic loss of *TET1* (Figure 4B and Supplementary Table S3; *P*= 0.0011).

In *IDH*-wt GBM, bi-allelic *TET1* loss (CNR <0.5) was enriched in patients with *EGFR* amplification (Figures 3 and 4C). No associations were observed with other frequently affected genes such as *TP53, CDKN2A/B*, or *TERT*p (Figure 3). Likewise, no significant correlations of bi-allelic *TET1* loss with clinical parameters including age, tumor size and Ki67 value were observed. Interestingly, bi-allelic *TET1* deletions were not associated with global concentrations of 5hmC (ranging between 0% and 1% of genomic DNA) or 5mC (accounting for 3%–4% of gDNA) in *IDH*-wt GBM (Figure 4D). Likewise, no significant differences of 5mC/5hmC levels were detected between *IDH*-wt and *IDH*-mutated tumors (Fig S4).

However, the genomic loss of *TET1* was associated with reduced levels of *TET1* mRNA expression in tumors with mono-allelic (relative expression ~24%) and bi-allelic (relative expression ~15%) *TET1* deletions, compared to control samples (*TET1*-wt; Figure 4E). In addition, there was a general trend toward higher concentrations of 5hmC with increasing levels of *TET1* mRNA expression (Figure 4F). With respect to outcome, genomic *TET1* loss and mRNA expression were not independent prognostic factors for PFS

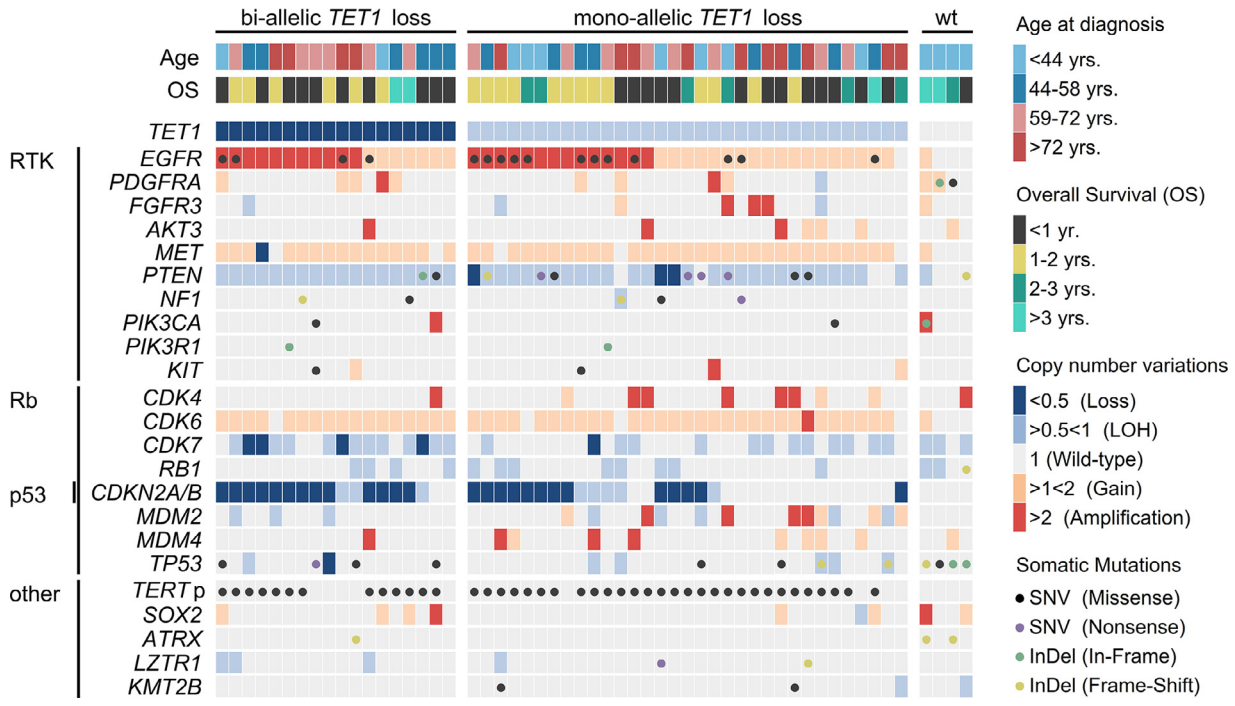

Figure 3. Somatic profiles of *IDH*-wt tumors with or without bi-allelic *TET1* loss. Distribution of somatic alterations (dots): missense single nucleotide variants (SNV; black), nonsense SNV (purple), in-frame (green) and frame-shift (yellow) insertion/deletion (InDel) mutations. Copy number variations (color coded by type) in relevant oncogenes related to RTK/Rb/p53 signaling pathways and clinical characteristics (age and overall survival) of 55 patients with *IDH*-wt GBM. *TET1* copy number ratios <0.5 are indicative for bi-allelic deletions in at least a subset of tumor clones and were classified "loss." Associated alterations are shown for patients with bi-allelic *TET1* loss, mono-allelic *TET1* deletion and *TET1* wild type status. The distribution of mutations in other putative oncogenes is presented in Figure S2.

and OS in our cohort. However, in patients with *EGFR* amplification, bi-allelic *TET1* loss (CNR <0.5) was significantly (P= 0.0303) associated with decreased OS (median OS = 12.4 mo) compared to patients with *TET1* CNRs >0.5 (median OS = 18.7 mo; Figure 4G).

Discussion

Frequent Genomic Loss of TET1 *in* IDH-*wt GBM*

In this study, we detected bi-allelic loss of *TET1* in 33% of patients in a minimal deleted region at 10q21.3, not previously described for GBM. Correspondingly, genomic *TET1* loss was associated with lower levels of *TET1* mRNA, demonstrating a reduced expression of *TET1* in these tumors. Interestingly, *TET1* expression in GBM with bi-allelic *TET1* loss was still ~15% of control samples without *TET1* copy number loss (wt), pointing to the presence of micromilieus and intratumoral heterogeneity with *TET1* mRNA expression at subclonal levels. Similarly, *TET1*CNRs of samples with bi-allelic *TET1* loss ranged between 0.23 and 0.49, which is indicative for complete genomic *TET1* inactivation in a subset of tumor clones. Subsequently, we show that genomic *TET1* deletions are frequent alterations primarily associated with *IDH*-wt GBM. In addition, *EGFR* amplification and bi-allelic *TET1* deletions co-occurred frequently, suggesting a functional interaction indicative of a distinct pathway of genesis in this subset of *IDH*-wt GBM. More importantly, although the presence of bi-allelic *TET1* deletions alone were not an independent prognostic factor, patients with mutual *TET1* loss and *EGFR* amplifications showed significantly worse outcomes compared with patients with only one or none of these alterations. In line, oncogenic *EGFR* amplifications were recently shown to induce silencing of tumor suppressor genes by repressing the DNA demethylase *TET1* in GBM cell lines [22]. Moreover, the latter work reported on a synergistic effect of TET1 in blocking tumor growth by modulating the response to *EGFR* inhibitors [22].

In addition to *EGFR* induced repression, the enzymatic inhibition of the TET proteins (TET1/2) via the production of 2-hydroxyglutarate (2HG) is a common mechanism in *IDH1*-mutated GBM, contributing to the establishment of the CIMP phenotype in proneural GBM [10]. However, while mutations of *TET2* are frequently associated with malignant progression in diverse cancers, so far, data on genomic alterations of *TET1* in cancer is scarce, except for a frequent DNA copy number loss of *TET1* recently reported in prostate cancer [13,14,23]. Notably, as no copy number alterations at 10q21.3 were detected in corresponding blood samples, the presence of germline aberrations or technical errors (e.g., insufficient enrichment or sequencing) can likely be excluded.

In GBM, TET1 was shown to play an important role in the tumorigenicity of GBM cells and to confer recruitment of the CHTOP-methylosome complex by the production of 5hmC [24,25]. Consistently, we show that concentrations of 5hmC were associated with levels of *TET1* mRNA expression in *IDH*-wt GBM. The key role of TET1 for active DNA demethylation in the adult brain via the conversion of 5mC to 5hmC at CpG islands has been previously described [12,26]. Unexpectedly, global concentrations of 5hmC (and 5mC) as measure for TET induced DNA demethylation, were not associated with bi-allelic *TET1* loss in our cohort. This is indicative for the presence of alternative mechanisms contributing to overall levels of 5hmC, like the activity of other enzymes involved in active DNA demethylation, namely TET2/3. For example, while TET1 mainly mediates the conversion of 5mC to 5hmC at CpG islands of gene promoters, TET2 and TET3 are involved in DNA demethylation of whole gene bodies (and intronic regions), which is significantly linked to overall cellular production of 5hmC [12,27]. In addition, 5hmC levels are likely affected by passive DNA demethylation in proliferating cells and/or the nuclear exclusion

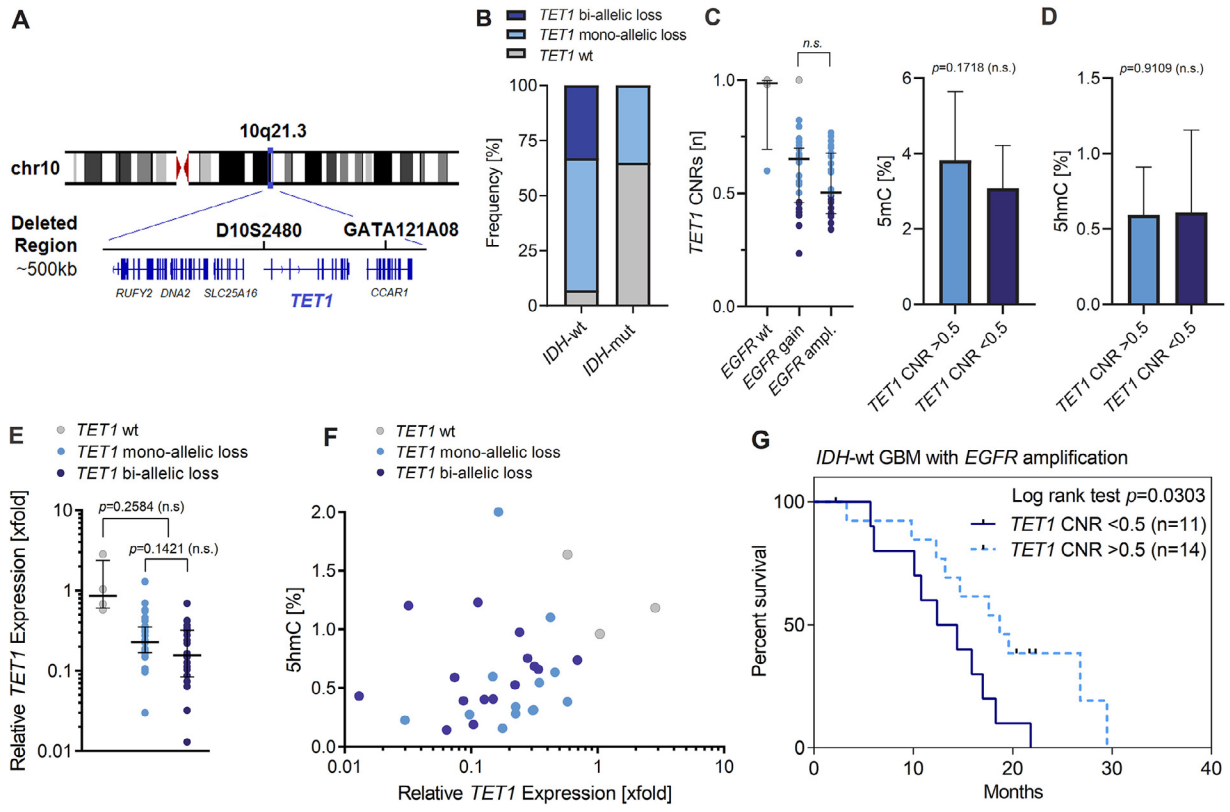

Figure 4. Molecular and clinical associations of genomic *TET1* loss. (A) Schematic illustration showing the position of acquired genomic deletion at 10q21.3 (chr10:70066243-70548143) covering a size of ~500 kb, affected genes (*RUFY2, DNA2, SLC25A16, TET1*, and *CCAR1*) and the position of short tandem repeat (STR) microsatellite loci D10S2480 and GATA121A08 used for *TET1* deletion mapping in *IDH*-wt and *IDH*-mutated GBM. (B) Frequency (%) of *TET1* deletion in *IDH*-wt and *IDH*-mutated GBM. (C) Association of *TET1* copy number ratios (CNRs) with *EGFR* amplification status. (D) Concentrations (% of gDNA) of 5-methylcytosine (5mC) and 5-hydroxymethylcytosine (5hmC) as measure for global DNA (de)methylation in *IDH*-wt GBM with mono-allelic (CNR >0.5) and bi-allelic (CNR <0.5) *TET1* deletion. (E) The mRNA expression level (2^ddCt) of *TET1* measured by qRT-PCR in samples with *TET1*-wt (n=4), mono-allelic *TET1* deletion (n = 33) and bi-allelic *TET1* loss (n = 18). Error bars indicate median values with interquartile range. Relative changes to *TET1*-wt gene expression was analyzed using the Delta-Delta-Ct algorithm. *GAPDH* expression was used as internal control. (F) Relative *TET1* expression [2^ddCt] and corresponding concentrations of global 5hmC (%) in patients with available 5hmC data (n = 31). (G) Kaplan-Meier analysis showing overall survival (mo) of patients affected by *EGFR* amplification and with (n = 11) or without (n = 14) concomitant bi-allelic loss (CNR <0.5) of the DNA demethylase *TET1*. Statistical associations were evaluated using the 2-sided Students t-test, the Mann-Whitney *U* test and the Mantel-Cox test. *P* values <0.05 were considered significant.

of the TET1 protein, as common feature in glioma cells [28]. Similarly, we did not see any significant differences of 5hmC concentrations in our *IDH1*-mutated GBM cohort, where genomic loss of *TET1* was detected with significantly lower frequencies. To fully understand functional and prognostic consequences of *TET1* deletion as potential therapeutic target in *IDH*-wt GBM, future investigations may specifically profile aberrant DNA methylation at CpG islands in relation to the genomic *TET1* loss and expression patterns.

Somatic Genomic Alterations of IDH-*wt GBM*

Mutations in our cohort which exclusively includes *IDH*-wt GBM were detected with a mean rate of 33 coding variants per tumor exome, corresponding to a frequency of ~1.2 somatic mutations per megabase, which is in the range of mutation frequencies previously reported for GBM [6,29]. In line with previous reports [5,6,30], 91% of patients were affected by mutations in classical GBM driver genes *TERT*p (C228T = 65%; C250T = 11%), *EGFR, TP53, PTEN* (all in 20%–30%), and *NF1* (9%), validating the sensitivity and comparability of our NGS results. Based on the integration of gene size calibrated (n Mb-1) mutation rates (Figure 1A; red dots), elevated numbers of variants in genes such as *TTN* (11%), *PCLO* (9%), *DNAH2/3* (7%), *RYR2* (7%), and *MUC16* (7%) detected in our cohort, likely represent random events (passenger mutations), due to the large genomic size of the respective genes [29]. Interestingly, no significant association with PFS or OS was observed for the integration of single recurrent oncogenes with outcome, including *TERT*p mutations which were previously associated with poor survival in primary GBM [7,30]. However, mutation rates of *TERT*p were lowest (62%) in younger patients <40 y, confirming an association of *TERT*p mutations with patients age and clinical performance, respectively [30]. The majority (7 out of 13) of patients without *TERT*p mutation harbored mutations in *TP53* and concomitant inactivating variants in the SWI/SNF complex gene *ATRX* (in 3 patients), likely representing an alternative mechanism of telomere lengthening in *TERT*p-wt GBM [6,11,30,31]. In total, 67% of patients carried amplifications in genes associated with RTK signaling (*EGFR, PDGFRA, AKT3, SOX2*), *TP53* induced apoptosis (*MDM2/4*) and/or cell cycle control via Rb signaling (*CDK4/6*), representing the 3 key regulatory pathways commonly altered in GBM [6]. *EGFR* amplification at high copy numbers was the most frequent alteration and closely associated with loss of *CDKN2A/B*, as described previously [6]. Within the RTK signaling

pathway, *EGFR* amplifications were detected almost mutually exclusive to other frequent RTK lesion (e.g., *PDGFRA* amplification), reflecting an alternative route of RTK-mediated clonal proliferation [6]. Although *EGFR* amplification generally confers a more aggressive phenotype, opposing implications were reported for clinical outcome [6–9,32]. In our study, *EGFR* amplification was significantly associated with higher rates of overall mutational burden and histopathological features of tumor aggressiveness, including tumor size, Ki67 values and poor long-term survival (>3y). This points to an increased genomic instability and tumor proliferation potential as a result of upregulated *EGFR* activity [8,9,32].

Conclusions

Bi-allelic deletions of the DNA demethylase gene *TET1* are frequent genomic events that co-occur with *EGFR* amplifications and are associated with reduced levels of *TET1* mRNA expression in *IDH*-wt GBM. Bi-allelic *TET1* loss was not associated with concentrations of 5hmC as measure for global DNA demethylation, suggestive for a site-specific effect of TET1 activity for DNA (de)methylation at specific genomic loci. Although bi-allelic *TET1* deletions were not an independent prognostic factor, they are associated with poor outcome in *IDH*-wt GBM harboring simultaneous *EGFR* amplification.

Authors' Contributions

Conception of the work: T.J., D.K., C.T.; Sample Collection: T.J., S.R., A.Z.; Aquisition/Analysis of Data: S.S., A.P., S.R., A.Z.; Bioinformatic Analysis: S.S., A.P., A.D.; Interpretation of Data: S.S., T.J., G.S., D.K., C.T.; Drafted the manuscript: S.S., T.J.; All Authors have seen and approved the manuscript being submitted.

Acknowledgement

For excellent technical assistance we thank Marita Hartwig, Marika Böhm, Katja Robel and Juliane Blaesche.

Supplementary Materials

Supplementary material associated with this article can be found, in the online version, at doi:10.1016/j.neo.2020.10.010.

References

[1] Alexander BM, Cloughesy TF. Adult Glioblastoma. *J Clin Oncol* 2017;**35**(21):2402–9.

[2] Shergalis A, Bankhead A 3rd, Luesakul U, Muangsin N, Neamati N. Current challenges and opportunities in treating glioblastoma. *Pharmacol Rev* 2018;**70**(3):412–45.

[3] Aldape K, Brindle KM, Chesler L, Chopra R, Gajjar A, Gilbert MR, Gottardo N, Gutmann DH, Hargrave D, Holland EC, et al. Challenges to curing primary brain tumours. *Nat Rev Clin Oncol* 2019;**16**(8):509–20.

[4] Szerlip NJ, Pedraza A, Chakravarty D, Azim M, McGuire J, Fang Y, Ozawa T, Holland EC, Huse JT, Jhanwar S, et al. Intratumoral heterogeneity of receptor tyrosine kinases EGFR and PDGFRA amplification in glioblastoma defines subpopulations with distinct growth factor response. *Proc Natl Acad Sci USA* 2012;**109**(8):3041–6.

[5] Louis DN, Perry A, Reifenberger G, von Deimling A, Figarella-Branger D, Cavenee WK, Ohgaki H, Wiestler OD, Kleihues P, Ellison DW. The 2016 World Health organization classification of tumors of the central nervous system: a summary. *Acta Neuropathol* 2016;**131**(6):803–20.

[6] Brennan CW, Verhaak RG, McKenna A, Campos B, Noushmehr H, Salama SR, Chin L. The somatic genomic landscape of glioblastoma. *Cell* 2013;**155**:462–77.

[7] Aldape K, Zadeh G, Mansouri S, Reifenberger G, von Deimling A. Glioblastoma: pathology, molecular mechanisms and markers. *Acta Neuropathol* 2015;**129**(6):829–48.

[8] Mirchia K, Sathe AA, Walker JM, Fudym Y, Galbraith K, Viapiano MS, Corona RJ, Snuderl M, Xing C, Hatanpaa KJ, et al. Total copy number variation as a prognostic factor in adult astrocytoma subtypes. *Acta Neuropathol Commun* 2019;**7**(1):92.

[9] Muñoz-Hidalgo L, San-Miguel T, Megías J, Monleón D, Navarro L, Roldán P, Cerdá-Nicolás M, López-Ginés C. Somatic copy number alterations are associated with EGFR amplification and shortened survival in patients with primary glioblastoma. *Neoplasia* 2020;**22**(1):10–21.

[10] Turcan S, Rohle D, Goenka A, Walsh LA, Fang F, Yilmaz E, Campos C, Fabius AW, Lu C, Ward PS, et al. IDH1 mutation is sufficient to establish the glioma hypermethylator phenotype. *Nature* 2012;**483**(7390):479–83.

[11] Liu XY, Gerges N, Korshunov A, Sabha N, Khuong-Quang DA, Fontebasso AM, Fleming A, Hadjadj D, Schwartzentruber J, Majewski J, et al. Frequent ATRX mutations and loss of expression in adult diffuse astrocytic tumors carrying IDH1/IDH2 and TP53 mutations. *Acta Neuropathol* 2012;**124**(5):615–625.

[12] Putiri EL, Tiedemann RL, Thompson JJ, Liu C, Ho T, Choi JH, Robertson KD. Distinct and overlapping control of 5-methylcytosine and 5-hydroxymethylcytosine by the TET proteins in human cancer cells. *Genome Biol* 2014;**15**(6):R81.

[13] Lian CG, Xu Y, Ceol C, Wu F, Larson A, Dresser K, Xu W, Tan L, Hu Y, Zhan Q, et al. Loss of 5-hydroxymethylcytosine is an epigenetic hallmark of melanoma. *Cell* 2012;**150**(6):1135–46.

[14] Ko M, Huang Y, Jankowska AM, Pape UJ, Tahiliani M, Bandukwala HS, An J, Lamperti ED, Koh KP, Ganetzky R, et al. Impaired hydroxylation of 5-methylcytosine in myeloid cancers with mutant TET2. *Nature* 2010;**468**(7325):839–43.

[15] Juratli TA, Kirsch M, Robel K, Soucek S, Geiger K, von Kummer R, Schackert G, Krex D. IDH mutations as an early and consistent marker in low-grade astrocytomas WHO grade II and their consecutive secondary high-grade gliomas. *J Neurooncol* 2012;**108**(3):403–10.

[16] Stasik S, Salomo K, Heberling U, Froehner M, Sommer U, Baretton GB, Ehninger G, Wirth MP, Thiede C, Fuessel S. Evaluation of TERT promoter mutations in urinary cell-free DNA and sediment DNA for detection of bladder cancer. *Clin Biochem* 2019;**64**:60–3.

[17] McKenna A, Hanna M, Banks E, Sivachenko A, Cibulskis K, Kernytsky A, Garimella K, Altshuler D, Gabriel S, Daly M, et al. The Genome Analysis Toolkit: a MapReduce framework for analyzing next-generation DNA sequencing data. *Genome Res* 2010;**20**(9):1297–303.

[18] Li H, Durbin R. Fast and accurate short read alignment with Burrows-Wheeler transform. *Bioinformatics* 2009;**25**(14):1754–60.

[19] Mermel CH, Schumacher SE, Hill B, Meyerson ML, Beroukhim R, Getz G. GISTIC2.0 facilitates sensitive and confident localization of the targets of focal somatic copy-number alteration in human cancers. *Genome Biol* 2011;**12**(4):R41.

[20] Wen PY, Macdonald DR, Reardon DA, Cloughesy TF, Sorensen AG, Galanis E, Degroot J, Wick W, Gilbert MR, Lassman AB, et al. Updated response assessment criteria for high-grade gliomas: response assessment in neuro-oncology working group. *J Clin Oncol* 2010;**28**(11):1963–72.

[21] Yushkevich PA, Piven J, Hazlett HC, Smith RG, Ho S, Gee JC, Gerig G. User-guided 3D active contour segmentation of anatomical structures: significantly improved efficiency and reliability. *Neuroimage* 2006;**31**(3):1116–28.

[22] Forloni M, Gupta R, Nagarajan A, Sun LS, Dong Y, Pirazzoli V, Toki M, Wurtz A, Melnick MA, Kobayashi S, et al. Oncogenic EGFR represses the TET1 DNA demethylase to induce silencing of tumor suppressors in cancer cells. *Cell Rep* 2016;**16**(2):457–71.

[23] Spans L, Van den Broeck T, Smeets E, Prekovic S, Thienpont B, Lambrechts D, Karnes RJ, Erho N, Alshalalfa M, Davicioni E, et al. Genomic and epigenomic analysis of high-risk prostate cancer reveals changes in hydroxymethylation and TET1. *Oncotarget* 2016;**7**(17):24326–38.

[24] Fu R, Ding Y, Luo J, Huang KM, Tang XJ, Li DS, Guo SW. Ten-eleven translocation 1 regulates methylation of autophagy-related genes in human glioma. *Neuroreport* 2018;**29**(9):731–8.

[25] Takai H, Masuda K, Sato T, Sakaguchi Y, Suzuki T, Koyama-Nasu R, Nasu-Nishimura Y, Katou Y, Ogawa H, Morishita Y, et al. 5-Hydroxymethylcytosine plays a critical role in glioblastomagenesis by recruiting the CHTOP-methylosome complex. *Cell Rep* 2014;**9**(1):48–60.

[26] Guo JU, Su Y, Zhong C, Ming GL, Song H. Hydroxylation of 5-methylcytosine by TET1 promotes active DNA demethylation in the adult brain. *Cell* 2011;**145**(3):423–34.

[27] Chen K, Zhang J, Guo Z, Ma Q, Xu Z, Zhou Y, Xu Z, Li Z, Liu Y, Ye X, et al. Loss of 5-hydroxymethylcytosine is linked to gene body hypermethylation in kidney cancer. *Cell Res* 2016;**26**(1):103–18.

[28] Müller T, Gessi M, Waha A, Isselstein LJ, Luxen D, Freihoff D, Freihoff J, Becker A, Simon M, Hammes J, et al. Nuclear exclusion of TET1 is associated with loss of 5-hydroxymethylcytosine in IDH1 wild-type gliomas. *Am J Pathol* 2012;**181**(2):675–83.

[29] Lawrence MS, Stojanov P, Polak P, Kryukov GV, Cibulskis K, Sivachenko A, Carter SL, Stewart C, Mermel CH, Roberts SA, et al. Mutational heterogeneity in cancer and the search for new cancer-associated genes. *Nature* 2013;**499**(7457):214–18.

[30] Killela PJ, Reitman ZJ, Jiao Y, Bettegowda C, Agrawal N, Jr Diaz LA, Friedman AH, Friedman H, Gallia GL, Giovanella BC, et al. TERT promoter mutations occur frequently in gliomas and a subset of tumors derived from cells with low rates of self-renewal. *Proc Natl Acad Sci USA* 2013;**110**(15):6021–6.

[31] Lee J, Solomon DA, Tihan T. The role of histone modifications and telomere alterations in the pathogenesis of diffuse gliomas in adults and children. *J Neurooncol* 2007;**132**(1):1–11.

[32] McNulty SN, Cottrell CE, Vigh-Conrad KA, Carter JH, Heusel JW, Ansstas G, Dahiya S. Beyond sequence variation: assessment of copy number variation in adult glioblastoma through targeted tumor somatic profiling. *Hum Pathol* 2019;**86**:170–81.